Effects of management thinning on CO_2 exchange by a plantation oak woodland in south-eastern England

M. Wilkinson[1], P. Crow[2], E.L. Eaton[1] and J.I.L. Morison[1]

[1] Forest Research, Centre for Sustainable Forestry and Climate Change, Alice Holt Lodge, Farnham, Surrey, GU10 4LH, UK.

[2] Forest Research, Centre for Ecosystems, Society and Biosecurity, Alice Holt Lodge, Farnham, Surrey, GU10 4LH, UK.

Correspondence to: M. Wilkinson (matthew.wilkinson@forestry.gsi.gov.uk)

Abstract

Forest thinning, which removes some individual trees from a forest stand at intermediate stages of the rotation, is commonly used as a silvicultural technique and is a management practice that can substantially alter both forest canopy structure and carbon storage. Whilst a proportion of the standing biomass is removed through harvested timber, thinning also removes some of the photosynthetic leaf area and introduces a large pulse of woody residue (brash) to the soil surface which potentially can alter the balance of autotrophic and heterotrophic respiration. Using a combination of eddy covariance (EC) and aerial light detection and ranging (LiDAR) data, this study investigated the effects of management thinning on the carbon balance and canopy structure in a commercially managed oak plantation in the south-east of England. Whilst thinning had a large effect on the canopy structure, increasing canopy complexity and gap fraction, the effects of thinning on the carbon balance were not as evident. In the first year post thinning, peak summer photosynthetic rate was unaffected by the thinning, suggesting that the better illuminated ground vegetation and shrub layer compensated for the removed trees. Peak summer photosynthetic rate was reduced in the thinned area between 2009 and 2011 but there was no significant difference between sectors. Ecosystem respiration fluxes increased in the thinned relative to the unthinned area in the post thinning phase.

1 Introduction

In England, woodlands cover 10.0% of the land surface area, with the majority (0.78 Mha) comprising broadleaved woodland (Forestry Commission, 2013). The total carbon stock in the forest biomass was estimated to be 105.4 MtC in 2011 (Forestry Commission, 2014), with 27.7 and 77.7 MtC in conifer and broadleaved woodlands respectively. Much of this broadleaved woodland is in small areas, with 51% in woodlands < 20 ha (Forestry Commission, 2013) and a little more than half (57%) of these deemed to be under active management (Forestry Commission England, 2014). As forests are such large stores of carbon, the effects of disturbance (such as harvesting) are of considerable interest (e.g. Amiro et al., 2010). If more woodlands are brought back into management and thinning or felling is carried out, then the carbon balance may be affected.

Thinning is a forestry practice that aims to manage competition between trees in order to improve the quality, productivity, yield and form of the final tree crop, and to provide an economic return before final felling. In Britain, two main types of thinning are practised: low thinning and crown thinning, with intermediate thinning a combination of these. In low thinning, suppressed and sub-dominant trees are removed, along with those from the smaller diameter classes, thereby reducing the competition experienced by the larger, more valuable, trees. Crown thinning aims to reduce the competition from other larger trees (dominant and co-dominant). When trees of poorer growth are removed along with some dominant individuals to open the canopy, it can be classed as intermediate thinning (Kerr and Haufe, 2011).

A few studies have considered the impacts of thinning and other aspects of the forest management cycle on forest carbon balances using the eddy covariance technique (EC) (e.g. Vesala et al., 2005; Payeur-Poirier et al., 2011; Saunders et al., 2012). However, it is logistically challenging to manipulate forest stands at the scale required to facilitate EC studies. One approach is to thin the entire forest stand and analyse the pre- and post-thinning phases separately (e.g. Saunders et al., 2012), However, large inter-annual variation in forest C fluxes is common (e.g. Allard et al., 2008; Granier et al., 2008; Wilkinson et al., 2012) which makes unequivocal determination of the effect of thinning difficult from short time series. Alternatively, if only a portion of the forest stand is subjected to the thinning, contemporaneous treatment and control plots are possible, and paired EC systems may be used to detect the fluxes from each section, (e.g. Moreaux et al., 2011), although this approach requires extensive and homogeneous forest areas. For this study, neither of these approaches were available, and so the area and extent of the thinning operation was deliberately manipulated so that the EC tower was sited near to the line dividing the treatment and control portions of the forest.

Assessing the impacts of management thinning on the Net Ecosystem Exchange (NEE) of a forest stand is further complicated because NEE is the small difference between ecosystem respiration (R_{eco}) and Gross Primary Productivity (GPP), both of which are much larger components; a small shift in the balance between these will therefore have a large effect on NEE. Furthermore, the ways R_{eco} and GPP are affected by thinning will differ; for example, thinning changes the canopy density, altering the soil temperature and moisture conditions (e.g. Tang et al., 2005; Olajuyigbe et al., 2012) and affecting the soil component of R_{eco}. Vesala et al. (2005) found that whilst there was no reduction in the size of the carbon sink of a boreal Scots pine (*Pinus sylvestris* L.) stand in Finland following thinning, increases in ground vegetation photosynthesis and heterotrophic respiration were offset by decreases in canopy GPP and in both above- and below-ground autotrophic respiration. Amiro et al. (2010) published a comprehensive study tracking changes in net ecosystem productivity (NEP) across a variety of different forest types following a range of disturbance events. All three conifer forests studied that were subjected to thinning showed relatively short-term impacts on the carbon balance following a decrease in NEP in the year of disturbance. Other studies in managed forests have shown that NEP rates are sustained following thinning of canopy trees (e.g. Granier et al., 2008), which is often attributed to increased growth by sub-canopy plants after dominant canopy trees have been removed (Moreaux et al., 2011; Dore et al., 2012). Many of these studies are concerned with coniferous forests with very different seasonal dynamics to the deciduous oak woodland found in much of lowland England.

Aerial light detection and ranging (LiDAR) is a remote sensing method capable of producing three-dimensional models of large areas of landscape with sub-metre accuracy and has been used to measure forest height for more than a decade (e.g. Yu et al., 2003). In recent years, its application in forest inventories has become common practice, particularly in northern European countries, where the method is used to quickly cover large areas at a high spatial resolution (Næsset, 2004; Maier et al., 2006). Additionally, the ability to view the resulting data in a variety of ways removes the problems associated with illumination and shadowing seen with standard aerial photography. By carrying out aerial LiDAR surveys before and after a management thinning operation, it is possible to quantify the changes in the forest canopy structure.

The aim of this study was to examine the effects of management thinning on the factors determining the carbon balance of a plantation deciduous oak woodland in southern England. Our hypotheses were that the removal of pre-selected trees from the woodland during a thinning operation would lead to an initial reduction in GPP. As thinning also increases the amount of woody debris and other litter components added to the forest floor, an increase in R_{eco} was also expected. Together, these changes would result in a large decrease of NEE during the immediate period after thinning, which would be followed by a recovery of NEE to pre-thin rates over a period of time, possibly several years, although we could not predict the timescale.

2 Materials and Instrumentation

2.1 Site description

The eddy covariance measurement site is located in the Straits Inclosure, Alice Holt Research Forest, UK (51^{o} 09' N; 0^{o} 51' W), close to the Alice Holt Research Station in south-eastern England (Fig. 1a). The inclosure is a flat area with an elevation of 80 m above mean sea level; the surrounding landscape consists of mixed lowland woodland and both arable and pasture agricultural land. The whole 90 ha inclosure was planted in the 1820s with oak (Schlich, 1905) and then replanted in the 1930s. The main tree species is *Quercus robur* L., but other species, including European ash (*Fraxinus excelsior* L.), *Q. petraea* (Mattuschka) Liebl. and *Q. cerris* L., are present. There is a small area (4.6 ha) of mixed conifers consisting of Corsican pine (*Pinus nigra* subsp *laricio* Maire.) and Scots pine (*Pinus sylvestris* L.) at the north-west edge of the woodland and isolated pockets of Japanese red-cedar (*Cryptomeria japonica* (L.f.) D.Don) are also present in the eastern area. The understorey is dominated by hazel (*Corylus avellana* L.) and hawthorn (*Crataegus monogyna* Jacq.) (Pitman and Broadmeadow, 2001). Prior to this study, the whole of the stand was previously thinned in 1995.

The climate regime is mild temperate oceanic, the long term mean (1971-2000) screen annual air temperature was 9.6 ^{o}C and the mean annual precipitation 779 mm at the UK Meteorological Office affiliated weather station, Alice Holt, Farnham (51^{o} 10' N; 0^{o} 51' W), approximately 1.8 km from the measurement site. Further site-specific details can be found in Wilkinson et al. (2012).

Between June and August 2007, the eastern half of the woodland (approx. 47.5 ha) was selectively thinned (Fig. 1a) using an 'intermediate' thinning procedure, (see introduction) resulting in an open forest canopy with a uniform stand structure (Kerr and Haufe, 2011). Pre-selected trees (based on stem form and position within the canopy) were felled, de-limbed and sectioned using mechanical harvesters. The merchantable stem wood with a diameter > 7.0 cm was subsequently collected and transported to the forest roadside using a forwarder, before being removed from the forest by timber haulage lorries. This harvesting technique resulted in substantial disturbance to the understorey and shrub layer. Whilst all of the remaining woody debris was left on the site, some of it was collected and used to construct 'brash mats' for machinery movement in order to minimise damage and compaction to the soil, especially in areas of heavy traffic. Mensuration surveys carried out after the thinning in 2009 (western sector) and 2011 (eastern sector) showed 453 and 354 trees ha^{-1} respectively, a difference in stand density of approx 22% (Table 1).

2.2 Micrometeorological measurements and flux calculations

Eddy covariance (EC) measurements of energy flux (sensible and latent heat), momentum, net ecosystem exchange (NEE) and water vapour flux have been made above the forest canopy at the site since 1998. The flux tower is located close to the boundary of the thinned and un-thinned sectors (Fig. 1a). The EC instrumentation consisted of a three-dimensional sonic anemometer (model Solent R2 until September 2011, model Solent R3 thereafter, Gill Instruments, Lymington, UK) and a closed-path infrared CO_2 and H_2O analyser (model LI-6262 until October 2005, model LI-7000 thereafter, LI-COR Biosciences, Lincoln, Nebraska, USA), sampling air at 28 m height. Raw high frequency data (20.8 Hz) were logged using the Edisol software package (Moncrieff et al., 1997). Further details of the instrumentation can be found in Wilkinson et al. (2012). For that previous paper, post processing of the raw high frequency data was performed using the Edinburgh University micrometeorological software tool EdiRe (http://www.geos.ed.ac.uk/abs/research/micromet/EdiRe/); here we used the EddyPro software package (Ver 4.2.1, LI-COR Biosciences, Lincoln, Nebraska, USA) but with similar processing options. Angle of attack correction (specific to Gill anemometers) was applied according to Nakai et al. (2006). Double axis rotation tilt correction was also applied to ensure that the vertical velocity signal was orthogonal to the plane of mean air flow. The lag time of the sample from the intake point to the measurement cell of the infrared analyser was determined by maximising the covariance between the vertical wind velocity and scalar concentration. In order to account for flux loss caused by signal damping inside the tube, limited time response and sensor separation, etc, spectral corrections were applied using the fully analytical approach of Moncrieff et al. (1997). Following an analysis of night-time NEE dependence on friction velocity using the method described by Papale et al. (2006), night-time NEE data were rejected where friction velocity was less than a critical threshold (supplementary table 1). Since CO_2 profile data were not available for the entire measurement period, we have made no corrections for CO_2 storage below the EC instruments. Footprint analysis was performed based on the flux footprint model of Kljun et al. (2004) and the half-hourly flux measurements were rejected when more than 10% of the measured flux was derived from outside the woodland, our area of interest.

2.3 Flux data processing and treatment separation

Following the calculation of corrected NEE and in order to remove extreme spikes, which were assumed not to be biologically valid, a data filter was applied using an approach similar to that proposed by Papale et al. (2006) and Thomas et al. (2011). For each calendar year, NEE data were first split into positive or negative values. Positive values more than the mean positive value for the whole year plus three standard deviations were removed and the same approach applied to all negative values. A secondary stage data filter was subsequently applied, which removed positive values more than the mean monthly value for that half hourly period plus three standard deviations, and negative values less than the mean monthly value minus three deviations.

Thirty minute average flux data (including additional meteorological data such as air temperature, humidity and incident solar radiation (S_g)) were separated into two sectors according to wind direction: data that were collected when the wind direction was between 315° and 170° were classified as 'east sector' (the area that was thinned in 2007), and data collected when the wind direction was between 170° and 315° were classified as 'west sector' (unthinned area). Table 2 summarises the data availability after this classification into the two sectors. Ecosystem respiration (R_{eco}) was calculated for each sector using the method proposed by Reichstein et al (2005). Here each dataset was split into ten-day consecutive periods and R_{eco} was estimated using the Lloyd-Taylor regression model (Lloyd and Taylor, 1994) between night time CO_2 flux (global solar radiation < 20 W m^{-2}) and air temperature. The estimated value of R_{eco} was then assigned to the central time point of the averaging interval and linearly interpolated between time points.

2.4 Model parameters

In order to examine changes in the physiological drivers of the carbon balance, original quality controlled daytime and night-time 30 minute average NEE data were separated and analysed independently. The temperature sensitivity of ecosystem respiration for each sector of the forest was determined using an exponential equation fitted to the average half hourly night-time NEE and air temperature for each corresponding period:

$$\mathrm{R_s} = K_1 \exp(K_2 T_{air}) \qquad (1)$$

where $\mathrm{R_s}$ is the night-time NEE and T_{air} is the night-time air temperature at 26 m. Data fitted to this function were limited to night-time condition only where the mean half hourly $Sg < 20$ W m^{-2} and the quality control flag calculated by EddyPro according to the Mauder and Foken (2004) method was equal to zero.

The relationship between summer (July and August) daytime NEE and S_g was modelled using a rectangular-hyperbolic function:

$$\mathrm{NEE} = \left[\frac{(\varepsilon \cdot F^{\infty} \cdot S_g)}{(\varepsilon \cdot S_g + F^{\infty})} \right] + \mathrm{R_d} \qquad (2)$$

Where F^{∞} is the asymptotic net CO_2 assimilation rate, ε is the initial slope of the light response curve, and $\mathrm{R_d}$ is respiration in the dark. Data fitted to the light response model were limited to periods where the quality control flag (Mauder and Foken, 2004) was equal to zero.

2.5 LiDAR measurements and calculation of vegetation structure

The aerial photograph taken after thinning (Fig. 1a) and mensuration surveys revealed substantial spatial heterogeneity within the forest block and showed large differences in forest structure between the two sectors. Changes in canopy top height and gap fraction were assessed using aerial LiDAR surveys conducted over two flight campaigns for the whole of Alice Holt forest (800 ha) by the Unit for Landscape Modelling (ULM), (Dept. of Geography, University of Cambridge). The first was in early November 2006, prior to the thinning and the second in August 2009, two years after the thinning. Due to the mild autumn in 2006 both surveys were completed whilst the forest had a fully developed canopy. A LiDAR system (ALTM 3033, Optech Incorporated, Ontario, Canada) flown at an altitude of 1000 m above ground level and with a scan angle +/- 15° was used along a series of overlapping transects designed to cover the whole forest. The system combined a pulse rate of 33 kHz and an overlap of 50% between swaths, resulting in a point density of 2 to 4 points m^{-2}, which was used to generate a virtual cloud of 3D data points with an accuracy of +/- 15 cm root mean square (RMS). The first and last pulse return data were used to generate a Digital Surface Model (DSM) which included the tree cover and a Digital Terrain Model (DTM) representing the ground surface. These data were provided by the ULM as raster elevation models with a 0.5 m cell size. By subtracting the DTM from the DSM using GIS software (ArcGIS 10, Esri, Redlands, California, USA), Canopy Height Models (CHM) for each survey were created. Furthermore, by subtracting the 2006 DSM from the 2009 DSM, a model of change between the two surveys was also created (Fig. 1b).

To allow a detailed analysis of the vertical change in forest height and gap frequency between 2006 and 2009, each CHM was converted to a 1m cell size and then spatially split into a 1 ha grid. Canopy top height histograms (bin size = 50 cm) were calculated for each grid cell, based on the 10,000 values per hectare. Frequencies were then averaged for all the grid cells within each sector. Grid cells at the interface between the east and west areas of the forest were excluded from the analysis, as were those cells that contained, either wholly or partially, areas of the surrounding agricultural land. All analyses were conducted using R software (R Development Core Team, 2011).

3 Results

3.1 Climatic conditions

The prevailing wind direction at the site is from the south west, so more of the data come from periods when the wind is from the west sector (Table 2). As the meteorological conditions associated with easterly and westerly winds differ, the flux data recorded from the two sectors did not reflect the same meteorological conditions (Fig. 2). Mean canopy level annual air temperature (2004-2012) was slightly warmer when air flow was from the west sector (10.8 °C) than from the east sector (9.6 °C).

The mean diurnal course of air temperature over the bi-monthly winter periods of November - December and January - February were generally warmer when airflow was from the more usual west rather than the east. The largest difference in winter air temperature was observed in January - February 2012: a period of cold weather from the start of February, dominated by easterly conditions, persisted over the southern UK for about two weeks and was also associated with snowfall to parts of the region (Fig. 3a). Conversely, mean summer air temperatures (during daylight hours) were generally higher when airflow was from the east than from the west, as occurred in 2004. Incident solar radiation and relative humidity were generally very similar when air flow was from either sector (Fig. 2).

3.2 Variation in NEE

The mean diurnal course of NEE (Fig. 3b) indicated that the forest generally acted as a CO_2 source for the bi-monthly periods of November - December, January - February and March - April, although in exceptionally warm and early springs such as 2007 the forest became a weak CO_2 sink for a few hours around noon. Both sectors of the forest were a strong CO_2 sink from May through to October, although there was considerable variation between years. In some periods, when temperature and insolation conditions were very similar for each sector, NEE patterns were also similar (e.g. May - June 2007, and March - April, 2012). In other periods with similar temperature and insolation, NEE was different, for example, in July - August 2012.

3.3 Effects of thinning on ecosystem respiration

As expected for a temperate, deciduous forest, there was a large annual cycle in R_{eco}, with a peak in May - August, (Fig. 4a - 4c) but varying substantially year to year. Before thinning, annual R_{eco} patterns were similar between sectors (e.g. Fig. 4a, 2006) but in the immediate period after thinning R_{eco} was usually higher in the east sector (e.g. Fig. 4b, 2009), particularly in the warmer summer period. As weather conditions differed for fluxes measured for east and west, we compared the underlying relationships of R_{eco} with temperature between sectors.

As an assessment of the sensitivity of R_s to air temperature using the coefficients of the exponential function (Eq.(1)) revealed differences between sectors (Table 3). Overall Q_{10} was generally higher and more variable between years, when airflow was from the west sector (mean = 2.92; SD = 0.74) than from the east (mean = 2.08; SD = 0.23) however this was not the case in 2009 and 2010. The largest differences in R_s (highest in the east) between the two sectors occurred in 2009, two years after the thinning. This was the only year during which there was a constant small (although non-signifiant) positive offset in the sensitivity of R_s to air temperature between the two sectors (Fig. 4h).

3.4 Effects of thinning on canopy NEE light response

The asymptotic net CO_2 assimilation rate (F^{∞}) and apparent quantum yield (ε) were determined from a light response function (Eq.(2)) fitted to the summer (July and August) daytime NEE flux data for both forest sectors. Differences in F^{∞} were observed between the east and west sectors both before and after thinning (data not shown). Although both sectors followed the same general inter-annual pattern, there was no clear change (in either sector) after thinning. The magnitude of F^{∞} was generally larger than the maximum observed rates of daytime NEE, due to an over estimation of F^{∞} by the rectangular-hyperbolic model, therefore NEE at S_g 800 Wm^{-2} (NEE$_{800}$) was considered a better indication of the maximum rate of light saturated NEE. NEE$_{800}$ was consistently lower in the fluxes observed from the east sector (Fig. 5a) than from the west for the entire measurement period, there was no significant reduction in NEE$_{800}$ in 2008 in fluxes from either sector. Prior to 2007, the magnitude of apparent quantum yield (Fig. 5b) was generally higher when fluxes were from the west than from the east; the two sectors converged in the post thinning phase. R_d (respiration in the dark) estimated from the light response curves increased in the east sector post thinning relative to the west and remained higher through to 2012 (Fig. 5c) confirming the results of R_{eco} estimated using the Reichstein et al (2005) method.

3.5 Changes in canopy height and gap fraction

The canopy top height derived from the first return data from the LiDAR survey showed that the two sectors of forest had similar canopy height distributions in 2006, before thinning (Fig. 6a & b), but with some differences in detail. The small peak in frequency between 5 and 10m height in the west in 2006 (Fig. 6a) is from areas of the forest which were undergoing succession development following previous disturbance events. By 2009 these areas of the forest had grown and are evident as heterogeneous patches in Fig. 1b. In both sectors, the canopy height distribution profile changed, in the west this was because of growth, whilst in the east the thinning operation had a substantial effect. Prior to the thinning both maximum and mean canopy heights were similar in both sectors (Table 4). Between 2006 and 2009, the maximum canopy height increased in the west sector by 0.9 m, but was reduced slightly in the east sector by 0.1 m. Over the same time period mean canopy top height also increased in the west sector by 0.95 m and reduced in the east sector by 1.4m.

Changes in the canopy height distribution profiles were also observed (Fig. 6c & d). The elevation relief ratio, E (Pike and Wilson, 1971) reflects the degree to which the outer canopy surfaces are in the upper (E > 0.5) or lower (E < 0.5) portion of the height range is defined as:

$$\mathrm{E} = \frac{h_{\mathrm{mean}} - h_{\mathrm{min}}}{h_{\mathrm{max}} - h_{\mathrm{min}}} \quad (3)$$

where h_{mean}, h_{min}, and h_{max} are the mean, minimum and maximum canopy heights respectively. E was reduced substantially in the east because of the larger proportion of lower top heights, while there was only a small increase in E in the west (Table 4). The canopy top height distribution also showed a relatively small increase in the proportion of canopy > 15 m in height between 2006 and 2009 in the west (+ 6.2%) but a substantial reduction in the east (- 13.7%) as a result of the thinning operation.

The LiDAR survey also showed that canopy complexity across the upper-most surface of the forest in the east sector increased following the thinning operations. The relative variability in canopy height (indicated by the coefficient of variation) increased substantially (Table 4) in the east but not in the west. After thinning there was a large increase in the frequency of gaps in the forest canopy (canopy top height < 1 m) in the east sector but not the west, because of the removal of canopy trees (compare Fig. 6d). Gaps in the forest canopy were relatively uniformly distributed throughout the whole east sector and increased from a total area of 1.13 ha (3.1 % of the eastern area) in 2006 to 2.16 ha (6.6 %) in 2009. Over the same period there was a small decrease in the total area of gaps in the forest canopy in the west, which measured 0.89 ha (2.47% of the total western area) in 2006 and 0.85 ha (2.35%) in the 2009 surveys (Fig. 1b).

4. Discussion

Surprisingly, effects of the thinning procedure in 2007 on carbon balance were not clearly evident. In part, this might have been because of our experimental approach. We used eddy covariance measurements at one location near the boundary between the thinned and unthinned sectors in order to determine the CO_2 fluxes, because of the relatively small size of the forest block and being restricted to only one tower and EC system. The effects of thinning are partly obscured by: a) the differences in weather conditions when airflow is from either sector (Fig. 2); b) existing heterogeneity in fluxes from different parts of the forest prior to thinning (Fig. 3b) and d) the limited data availability for each sector (Table 2).

The pre- and post-thinning LiDAR surveys indicated that whilst canopy top height distributions were comparable in 2006, the thinning operations in 2007 had a large effect on the canopy structure of the east sector, resulting in a more complex canopy with a wider range of top heights and a larger total area of gaps. The complexity of the forest canopy at our site, as a result of variability in gaps and a dense understorey, contrasts with other published studies using LiDAR at other deciduous forest sites (Wasser et al., 2013). Whilst we acknowledge that the 2009 LiDAR survey was not immediately after the thinning, our estimate of the change in canopy gap fraction may be an under representation. Firstly, LiDAR pulses have a relatively large footprint (~25 cm in diameter) and therefore gaps in the canopy would need to be larger than this in order to be recognised as a gap. Secondly, off-nadir pulses are more likely to produce a canopy height return than they are to penetrate to ground level. Our approach used only the first and last return signals of the LiDAR data, so the canopy height model showed only the uppermost component of the forest canopy. As such, some of the changes in the understorey canopy during thinning may have been masked by the vertical overlap of the understorey vegetation and upper canopy. Whilst we acknowledge that an analysis of full wave-form or multiple return data (Mallet and Bretar, 2009) may provide more detailed information about the canopy's 3D structure, we maintain that the approach adopted here provided a useful assessment of the changes to the forest canopy due to the thinning operations.

The parameters obtained from the summer light response curves did not support our hypothesis that tree thinning would lead to a reduction in NEE through a loss of canopy photosynthetic area. Contrary to expectation, there was no clear difference in NEE_{800} (Fig.5) in 2008 for the east sector relative to the west. We suggest that this apparent insensitivity in 2008 to the thinning indicates that in the first year after thinning the newly exposed ground vegetation and shrub layer, and better illumination of the remaining crowns compensates for the removed trees. From 2009 to 2011, NEE_{800} was reduced in both sectors probably as a result of defoliation by caterpillars (Wilkinson et al., 2012). The increase in ε in the east in 2008 and especially 2009 may be as a result of the thinning as it consistent with the earlier work of Niinemets (2007) and Pangle et al. (2009) who demonstrated that as forest canopies become more structurally diverse, light efficiency increases because of a more even distribution of radiation throughout the tree canopy and better light penetration to sub-canopy species with a higher ε. Our findings however contrast with results from thinning studies carried out on evergreen conifer sites (with presumably little or no understorey vegetation). For example, Saunders et al. (2012) attributed observed changes in the photosynthetic efficiency of a Sitka spruce stand following thinning to inherent change in the photosynthetic efficiency of the remaining trees, rather than being due to increased light absorption.

The impacts of thinning on respiration are complicated by the fact that R_{eco} consists of CO_2 derived from both heterotrophic respiration (R_h) largely in the soil and from autotrophic respiration (R_a), both above and below ground. Both of these CO_2 sources comprise a number of processes and components which are likely to be influenced by both time and forest management in different ways. R_d estimated from the light response curves increased in the first years after thinning in the east relative to the west. In the first years' after thinning (2008 - 2010) the initial supply of fine roots, small twigs, leaves and other easily degradable fractions of litter would be a major new source of carbon and nitrogen for the decomposition system. Soil disturbance from machinery might also be expected to increase R_h as was demonstrated by Concilio et al. (2005) at a mixed species conifer site. In addition, much of the large woody debris had been gathered together to form brash mats which may have been a substantial source of CO_2, although we have no independent measurements of emission from them. Thinning is also likely to cause local increases in temperature, increased throughfall, reductions in humidity and probably higher evaporation rates in gaps (Vesala et al., 2005). However, we cannot quantify such effects as the climatic data we recorded was only that from the central instrument tower. After thinning there is likely to be a succession of changes in the relative contributions of R_a and R_h to total R_{eco}, which may be associated not only with changes to soil conditions but also with biomass removal (Anderson-Teixeira et al., 2011) and a reduction in GPP (Woodward et al., 2010). Although we do not have independent measures for R_a and R_h throughout the period of the present study, work at the site in 2008-2010 (Heinemeyer et al., 2012) demonstrated that in an unthinned area the largest proportion of total soil efflux was from R_a (56%) compared with R_h (44%). Importantly for this study, Heinemeyer et al. (2012) demonstrated a stronger temperature response for R_h than for either R_a (roots) or R_a (mycorrhizae). After thinning the proportion of total soil CO_2 efflux derived from R_h is likely to increase, which may result in an increased temperature sensitivity of CO_2 efflux by forest soils. In 2011 there was no clearly discernable difference in R_{eco} between the two sectors, and we therefore assume that any increase in below ground R_h is likely to be cancelled out by a corresponding reduction in R_a, which is consistent with the findings of Tang et al. (2005).

In a previous paper describing the pattern of CO_2 fluxes at this site between 1999 and 2010 (Wilkinson et al., 2012) we noted the substantial inter-annual variation in NEE. The analysis presented here (e.g. Fig. 3) suggest that part of that may be caused by inter-annual differences in the contribution from the east and west areas of the forest, which differed even before the thin.

5. Conclusion

This study has investigated the effects of management thinning on the carbon balance of deciduous oak woodland in south-eastern England. LiDAR data were used to assess changes in the forest canopy, while EC was used to measure changes in the carbon balance. Management thinning reduced the mean canopy top height and resulted in a forest canopy with a wider top height range and more gaps. The impacts of management thinning on the carbon balance were not clearly evident although ecosystem respiration was higher in fluxes from the east sector from 2008 onwards and remained higher until the end of the study period. The insensitivity of the summer photosynthetic parameters in the first year after thinning, 2008, suggests that newly exposed ground vegetation and shrub layers receiving better illumination compensated for the removed trees.

Acknowledgements

This work was funded by the Forestry Commission, and this paper is an output of the Managing Forest Carbon Programme. We are grateful to the local Forestry Commission staff for allowing and facilitating the research in the Straits Inclosure. We are indebted to Bernard Devereux, Gabriel Amable and Ed Wyer from the Unit of Landscape Modelling, Cambridge University for acquiring and processing the LiDAR data. We wish to acknowledge the help of many Forest Research colleagues who have helped on this work over the years, and particularly Mark Broadmeadow who initiated the project and set up the eddy covariance CO_2 flux site.

References

Allard, V., Ourcival, J. M., Rambal, S., Joffree, R., and Rocheteau, A.: Seasonal and annual variation of carbon exchange in an evergreen Mediterranean forest in southern France, Glob. Change Biol., 14, 714–725, 2008.

Amiro, B.D., Barr, A.G., Barr, J.G., Black, T.A., Bracho, R., Brown, M., Chen, J., Clark, K.L., Davis, K.J., Desai, A.R., Dore, S., Engel, V., Fuentes, J.D., Goldstein, A.H., Goulden, M.L., Kolb, T.E., Lavigne, M.B, Law, B.E., Margolis, H.A., Martin, T., McCaughey, J.H., Misson, L., Montes-Helu, M., Noormets, A., Randerson, J.T., Starr, G. and Xiao, J.: Ecosystem carbon dioxide fluxes after disturbance in forests of North America, J. Geophys Res-Atmos**.**, 115, G00K02, 2010.

Anderson-Teixeira, K., Delong, J., Fox, A., Brese, D., and Litvak, M.: Differential responses of production and respiration to temperature and moisture drive the carbon balance across a climatic gradient in New Mexico, Glob. Change Biol., 17, 410–424, 2011.

Concilio, A., Chen, J., Ma, S., and North, M.: Precipitation patterns drive inter-annual variation in summer soil respiration in a Mediterranean-climate, mixed conifer forest, Climatic Change., 92, 109-122, 2009.

Dore, S., Montes-Helu, M., Hart, S.C., Hungate, B.A., Koch, G.W., Moon, J.B., Finkral, A.J., and Kolb, T.E.: Recovery of ponderosa pine ecosystem carbon and water fluxes from thinning and stand-replacing fire, Glob. Change Biol., 18, 3171–3185, 2012.

Forestry Commission. NFI 2011 Woodland Map: National Forest Inventory Report. Forestry Commission, Edinburgh, 2013.

Forestry Commission. Carbon in live woodland trees in Britain: National Forest Inventory Report. Forestry Commission, Edinburgh. 2014.

Forestry Commission England. Corporate Plan Performance Indicators: Headline Performance Update 30 June 2014. Forestry Commission England, Bristol, 2014.

Granier, A., Bréda, N., Longdoz, B., Gross, P., and Ngao, J.: Ten years of fluxes and stand growth in a young beech forest in North Eastern France (Hesse Forest), Annals of Forest Science., 65, 704, 2008.

Heinemeyer, A., Wilkinson, M., Vargas, R., Subke, J.-A., Casella, E., Morison J.I.L., and Ineson, P.: Exploring the “overflow tap” theory: linking forest soil CO_2 fluxes and individual mycorrhizosphere components to photosynthesis, Biogeosciences, 9, 79-95, 2012.

Kerr, G. and Haufe, J.: Thinning Practice: A Silvicultural Guide. Forestry Commission, Edinburgh, 2011.

Kljun, N., Calanca, P., Rotach, M.W. and Schmid, H.P.: A simple parameterisation for flux footprint predictions, Bound-Lay Meteorol., 112, 503-523, 2004.

Maier, B., Tiede, D., Dorren, L.:Assessing mountain forest structure using airborne laser scanning and landscape metrics, in: Lang, S., Blaschke, T., Schöpfer, E. (Eds), Bridging Remote Sensing and GIS: 1st International Conference on Object-Based Image Analysis (OBIA 2006), Salzburg, 4-5 July 2006. Salzburg University, Austria, 2006.

Mallet, C. and Bretar, F.: Full-waveform topographic lidar: state-of-the-art. ISPRS J. Photogramm. Remote Sens., 64, 1-16, 2009.

Mauder, M. and Foken, T.: Impact of post-field data processing on eddy covariance flux estimates and energy balance closure, Meteorol. Z., 15, 597-609, 2006.

Moncrieff, J. B., Massheder, J. M., de Bruin, H., Elbers, J., Friborg, T., Heusinkveld, B., Kabat, P., Scott, S., Soegaard, H., and Verhoef, A.: A system to measure surface fluxes of momentum sensible heat, water vapour and carbon dioxide, J. Hydrol., 188-189, 589-611, 1997.

Moreaux, V., Lamaud, É., Bosc, A., Bonnefond, J.-M., Medlyn, B.E., and Loustau, D.: Paired comparison of water, energy and carbon exchanges over two young maritime pine stands (*Pinus pinaster* Ait.): effects of thinning and weeding in the early stage of tree growth, Tree Physiol., 31, 903-921, 2011.

Nakai, T., van der Molen, M.K., Gash, J.H.C., and Kodama, Y.: Correction of sonic anemometer angle of attack errors, Agric. Forest. Meteorol., 136, 19-30, 2006.

Næsset, E.: Accuracy of forest inventory using airborne laser scanning: evaluating the first Nordic full-scale operational project, Scand. J. Forest. Res., 19, 554-557, 2004.

Niinements, Ü.: Photosynthesis and resource distribution through plant canopies, Plant Cell Environ, 30, 1052–1071, 2007.

Olajuyigbe S., Tobin, B., Saunders, M., and Nieuwenhuis, M.: Forest thinning and soil respiration in a Sitka spruce forest in Ireland, Agric. Forest. Meteorol., 157, 86-95, 2012.

Pangle, L., Vose, J.M., and Teskey, R.O.: Radiation use efficiency in adjacent hardwoods and pine forests in the southern Appalachians. Forest. Ecol. Manag., 257, 1034-1042, 2009.

Papale, D., Reichstein, M., Aubinet, M., Canfora, E., Bernhofer, C., Kutsch, W., Longdoz, B., Valentini, R., Vesala, T., and Yakir, D.: Towards a standardized processing of NetEcosystem Exchange measured with eddy covariance technique algorithms and uncertainty estimation, Biogeosciences, 3, 571-583, 2006.

Payeur-Poirier, J.-L., Coursolle, C., Margolis, H.A., and Giasson, M.-A.: CO_2 fluxes of a boreal black spruce chronosequence in eastern North America. Agric. Forest. Meteorol., 153, 94-105, 2012.

Pike, R.J. and Wilson, S.E.: Elevation-relief ratio, hypsometric integral and geomorphic area-altitude analysis, Geol. Soc. Am. Bull, 82, 1079-108, 1971.

Pitman, R. M. and Broadmeadow, M. S. J.: Leaf area, biomass and physiological parameterisation of ground vegetation of lowland oak woodland. Internal Report to PPD, Forestry Commission, Edinburgh., 2001.

R Development Core Team, 2011. R: A language and Environment for Statistical Computing. R Foundation for Statistical Computing, Vienna.

Reichstein, M., Falge, E., Baldocchi, D., Papale, D., Valentini, R., Aubinet, M., Berbigier, P., Bernhofer, C., Buchmann, N., Gilmanov, T., Granier, A., Grünwald, T., Havránková, K., Janous, D., Knohl, A., Laurela, T., Lohila, A., Loustau, D., Matteucci, G., Meyers, T., Miglietta, F., Ourcival, J. M., Rambal, S., Rotenberg, E., Sanz, M., Seufert, G., Vaccari, F., Vesala, T., and Yakir, D.: On the separation of net ecosystem exchange into assimilation and ecosystem respiration: review and improved algorithm, Global. Change. Biol., 11, 1-16, 2005.

Saunders, M., Tobin, B., Black, K., Nieuwenhuis, M., and Osborne, B.: Thinning effects on the net ecosystem carbon exchange of a Sitka spruce forest are temperature-dependent. Agric. Forest. Meteorol., 157, 1-10, 2012.

Schlich, W.: Working plan for the Alice Holt Forest, His Majesty's Stationery Office, London, 1905.

Tang, J., Qi, Y., Xu, M., Misson, L., and Goldstein, A.H.: Forest thinning and soil respiration in a ponderosa pine plantation in the Sierra Nevada, Tree Physiol., 25, 57-66, 2005.

Thomas, M. V., Malhi, Y., Fenn, K. M., Fisher, J. B. Morecroft, M. D., Lloyd, C. R., Taylor, M. E., and McNeil, D. D.: Carbon dioxide fluxes over an ancient broadleaved deciduous woodland in southern England, Biogeosciences, 8, 1595-1613, 2011.

Vesala, T., Suni, T., Rannik, Ü., Keronen, P., Markkanen, T., Sevanto, S., Grönholm, T., Smolander, S., Kulmala, M., Ilvesniemi, H., Ojansuu, R., Uotila, A., Levula, J., Mäkelä, A., Pumpanen, J., Kolari, P., Kulmala, L., Altimir, N., Berninger, F., Nikinmaa, E., and Hari, P.: Effect of thinning on surface fluxes in a boreal forest. Global Biogeochem. Cy, 19, GB2001, 2005.

Wasser, L., Day, R., Chasmer, L., and Taylor, A. Influence of vegetation structure on Lidar-derived canopy height and fractional cover in forested riparian buffers during leaf-off and leaf-on conditions. PLoS One, 8(1), e54776, 2013.

Wilkinson, M., Eaton, E. L., Broadmeadow, M. S. J., and Morison, J. I. L.: Inter-annual variation of carbon uptake by a plantation oak woodland in south-eastern England, Biogeosciences, 9, 5373-5389, 2012.

Woodward, I., Quaife, T., and Lomas, M.: Changing climate and the Irish landscape. Biol. Environ, 110, 1–16, 2010.

Yu, X., Hyyppä, J., Rönnholm, P. Kaartinen, H., Maltamo, M., and Hyyppä, H.: Detection of harvested trees and estimation of forest growth using laser scanning. In: Hyyppä, J., Næsset, E., Olsson, H., Grandqvist Pahlen, T., Reese, H. (Eds), Proceedings of Scandlaser Scientific Workshop on Airborne Laser Scanning of Forests, Umeå, 3-4 September 2003. Working Paper 112, pp. 115-124. Department of Forest Resource Management and Geomatics, Swedish University of Agricultural Science, 2003.

Table 1.

Results of tree mensuration surveys carried out in 2009 (west sector) and 2011 (east sector) at the Straits Inclosure, Alice Holt Forest. In the east sector 26 circular plots were measured each with a radius of 12.6 m, whilst in the west sector, 18 plots were measured each with a plot radius of 8 m. Plots locations were selected using a stratified grid basis to ensure the heterogeneity of the forest structure was measured; figures in brackets are standard error.

	All trees		Oak trees only	
	Density (trees ha^{-1})	Mean diameter at breast height (cm)	Density (trees ha^{-1})	Mean diameter at breast height (cm)
East	354	23.9 (0.55)	217	30.0 (0.53)
West	450	26.6 (0.57)	423	26.8 (0.57)

Table 2.

Annual eddy covariance CO_2 flux data capture and quality controlled data availability following de-spiking, footprint and u* quality checks for each sector by time of day (all in %) over the period 2004 - 2012 at the Straits Inclosure, Alice Holt Forest.

Year	Total data Capture	QC East day	QC East night	QC West day	QC West night
2004	79.6	8.9	6.1	18.7	14.7
2005	92.5	11.6	8.3	21.6	16.3
2006	74.3	10.7	8.6	16.6	11.4
2007	92.5	9.9	6.3	18.6	12.8
2008	81.4	10.7	6.4	26.0	21.o
2009	77.3	11.9	10.0	15.7	12.9
2010	93.0	15.9	10.5	18.9	14.1
2011	86.7	12.6	9.5	18.4	15.1
2012	82.1	11.9	8.6	18.0	14.9
Mean	84.4	11.6	8.3	19.2	14.8

Table 3.

Night-time ecosystem respiration (R_s) coefficients and the estimated Q_{10} values (base temperature = 0^{o}C) derived from fitting an exponential equation to half hourly night-time NEE and air temperature vales over the period 2004 - 2012 at the Straits Inclosure, Alice Holt Forest.

Year	K1 East	K2 East	K1 West	K2 West	Q10 East	Q10 west
2004	2.22 (0.07)	0.064 (0.003)	1.22 (0.06)	0.120 (0.003)	1.90	3.32
2005	2.14 (0.06)	0.063 (0.002)	1.59 (0.07)	0.091 (0.003)	1.88	2.48
2006	1.82 (0.07)	0.068 (0.003)	1.67 (0.08)	0.082 (0.003)	1.97	2.27
2007	2.08 (0.10)	0.061 (0.004)	1.11 (0.06)	0.122 (0.004)	1.84	3.39
2008	1.82 (0.07)	0.078 (0.003)	0.81 (0.04)	0.140 (0.003)	2.18	4.06
2009	1.71 (0.07)	0.089 (0.003)	1.37 (0.06)	0.089 (0.089)	2.44	2.44
2010	1.70 (0.05)	0.072 (0.002)	1.74 (0.05)	0.064 (0.002)	2.05	1.90
2011	1.62 (0.08)	0.071 (0.004)	1.15 (0.05)	0.098 (0.004)	2.03	2.66
2012	1.72 (0.08)	0.088 (0.004)	0.93 (0.05)	0.134 (0.004)	2.41	3.82

Figures inside brackets are one standard error (SE).

Table 4.

Results of aerial LiDAR surveys before and after thinning calculated from first and last return data at a point density of 2 points m^{-2} and extracted from a 1ha gridded canopy height model at the Straits Inclosure, Alice Holt Forest

Year	Sector	Maximum height (m)	Mean height (m)	S.D of mean height	C.V.	Elevation relief ratio (E)	% of canopy > 10m	% of canopy > 15m
2006	West	25.7	15.0	5.04	0.34	0.58	81.9	66.3
2006	East	26.0	15.0	5.03	0.34	0.57	84.5	65.3
2009	West	26.6	15.9	4.99	0.32	0.59	85.8	72.5
2009	East	25.9	13.6	6.19	0.46	0.52	73.6	51.7

Figure captions

Figure 1a. Aerial photograph (taken in spring 2008) of the Straits Inclosure, Alice Holt Forest. © Bluesky International Ltd/Getmapping PLC

Figure 1b. Change in canopy height between November 2006 and August 2009 calculated using aerial LiDAR data at the Straits Inclosure, Alice Holt Forest.

Figure 2. Average bi-monthly values (2004-2012) for the key climatic variables of (a) air temperature (b) incident solar radiation, *Sg* and (c) relative humidity for the east (blue) and west (green) sectors, error bars represent ± 1 standard deviation (n=7) at the Straits Inclosure, Alice Holt Forest.

Figure 3a. Average bi-monthly diurnal curve of incident solar radiation, S_g for east sector (blue solid line) and west sector (green solid line) and air temperature for east sector (blue open circles) and west sector (green open circles) for 2004, 2007 and 2012 at the Straits Inclosure, Alice Holt Forest.

Figure 3b. Mean bi-monthly diurnal curve of net ecosystem exchange for east sector (blue solid line) and west sector (green solid line) for 2004, 2007 and 2012, + symbols represent ± 1SE at the Straits Inclosure, Alice Holt Forest.

Figure 4. Monthly estimated R_{eco} for the east sector (blue solid line with open circles) and west sector (green solid line with open circles) for (a) 2006 (b) 2009 (c) 2012; monthly mean air temperature (at 26 m height) and monthly precipitation total for (d) 2006, (e) 2009 (f) 2012; modelled temperature response (R_s derived from night-time NEE fluxes only) for east sector (blue sold line) and west sector (green solid line) for (g) 2006 (h) 2009 (i) 2012, error bars represent 95% confidence intervals, at the Straits Inclosure, Alice Holt Forest.

Figure 5. Inter-annual variation in summer (July and August) daytime light response model parameters for (a) NEE_{800} (b) ε and (c) Rd for the east sector (blue line with open circles) and west sector (green line with open circles) error bars represent ± 1SE, at the Straits Inclosure, Alice Holt Forest.

Figure 6. Histograms of canopy top height (m) derived from aerial LiDAR for the east sector (blue bars) and west (green bars) for (a) 2006 and 2009 west sectors, (b) 2006 and 2009 east sectors, cumulative frequency of canopy top height for (c) west sector in 2006 & 2009 and (d) east sector in 2006 and 2009 at the Straits Inclosure, Alice Holt Forest.


N
W
E
S
Thinned
(East)
Flux tower
Unthinned
(West)
0
125
250
500 Metres

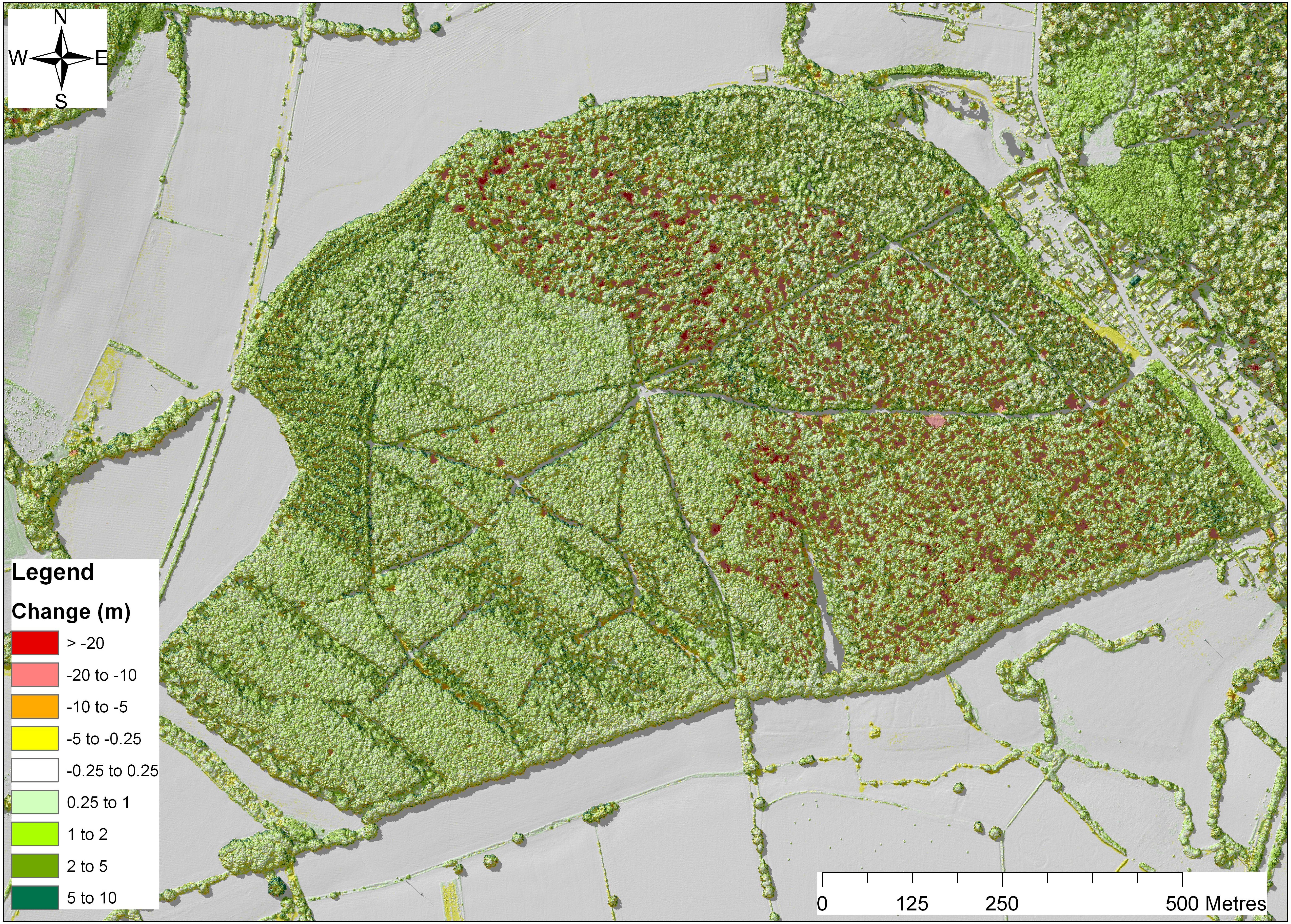
N
W
E
S
Legend
Change (m)
> -20
-20 to -10
-10 to -5
-5 to -0.25
-0.25 to 0.25
0.25 to 1
1 to 2
2 to 5
5 to 10
0
125
250
500 Metres

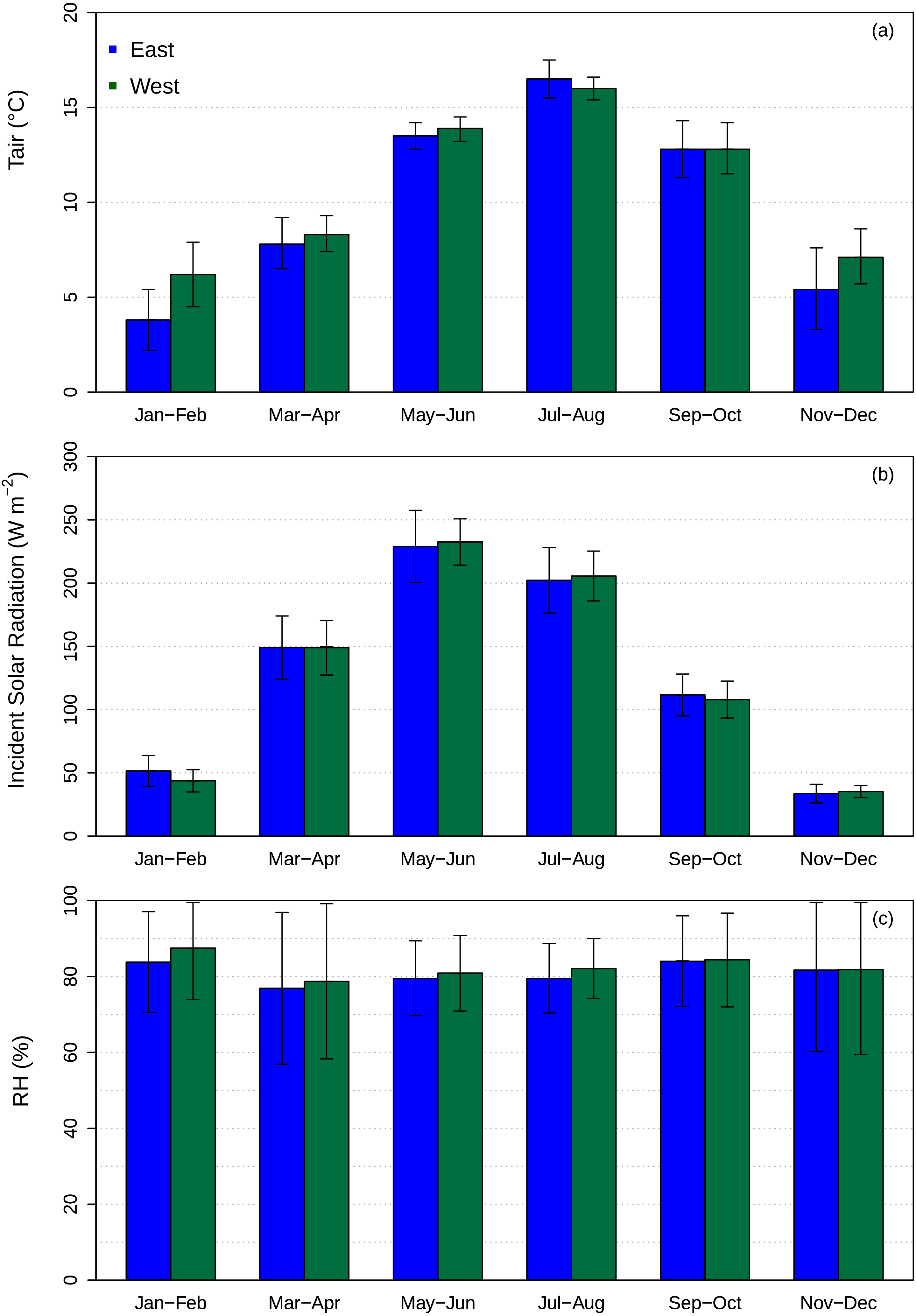

(a)
East
West
Tair (°C)
0
5
10
15
20
Jan−Feb
Mar−Apr
May−Jun
Jul−Aug
Sep−Oct
Nov−Dec
(b)
Incident Solar Radiation (W m^{-2})
0
50
100
150
200
250
300
Jan−Feb
Mar−Apr
May−Jun
Jul−Aug
Sep−Oct
Nov−Dec
(c)
RH (%)
0
20
40
60
80
100
Jan−Feb
Mar−Apr
May−Jun
Jul−Aug
Sep−Oct
Nov−Dec

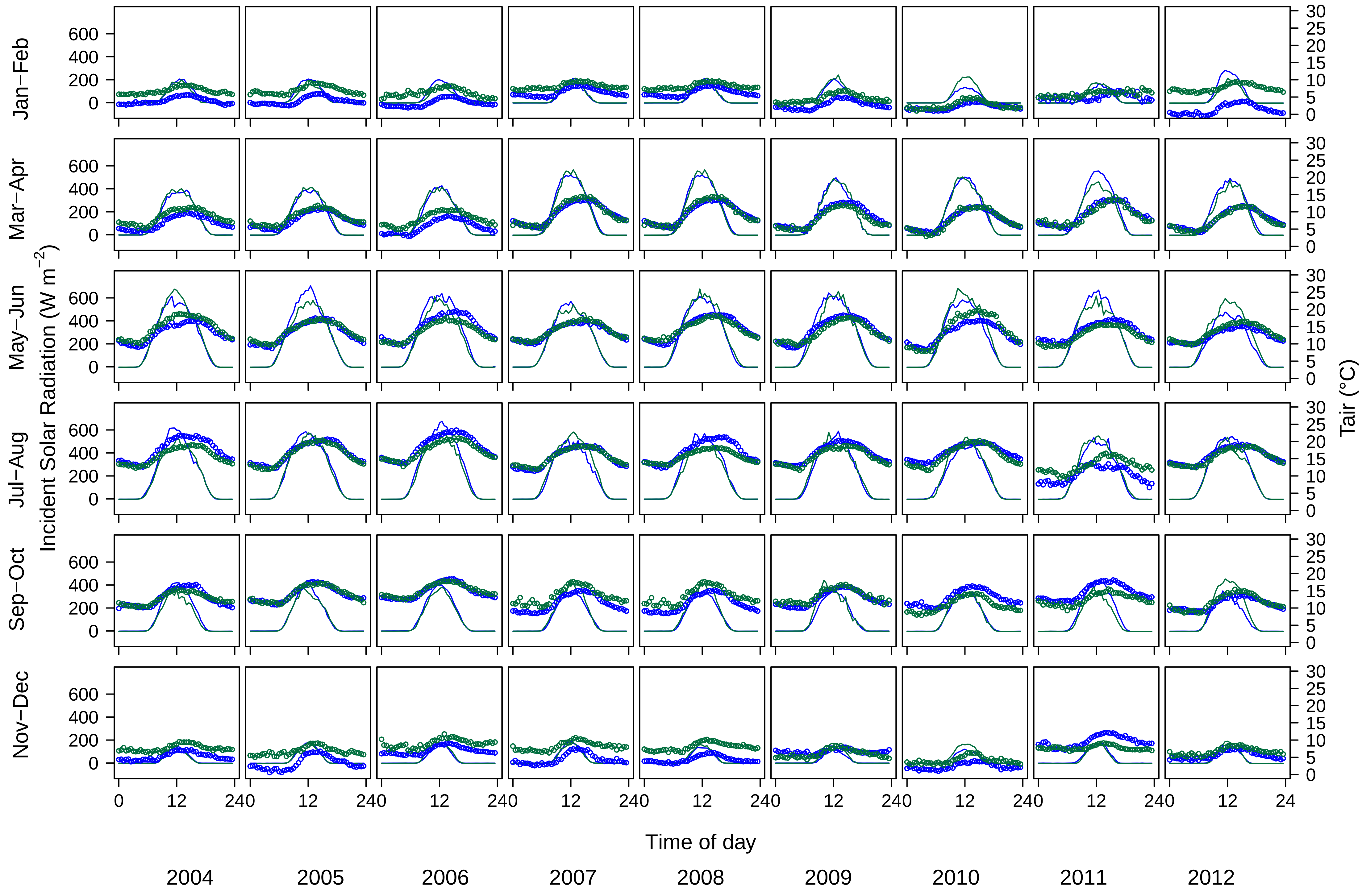

Jan−Feb
Mar−Apr
May−Jun
Jul−Aug
Sep−Oct
Nov−Dec
Incident Solar Radiation (W m^{-2})
Tair (°C)
Time of day
0
12
24
200
400
600
0
5
10
15
20
25
30
2004
2005
2006
2007
2008
2009
2010
2011
2012

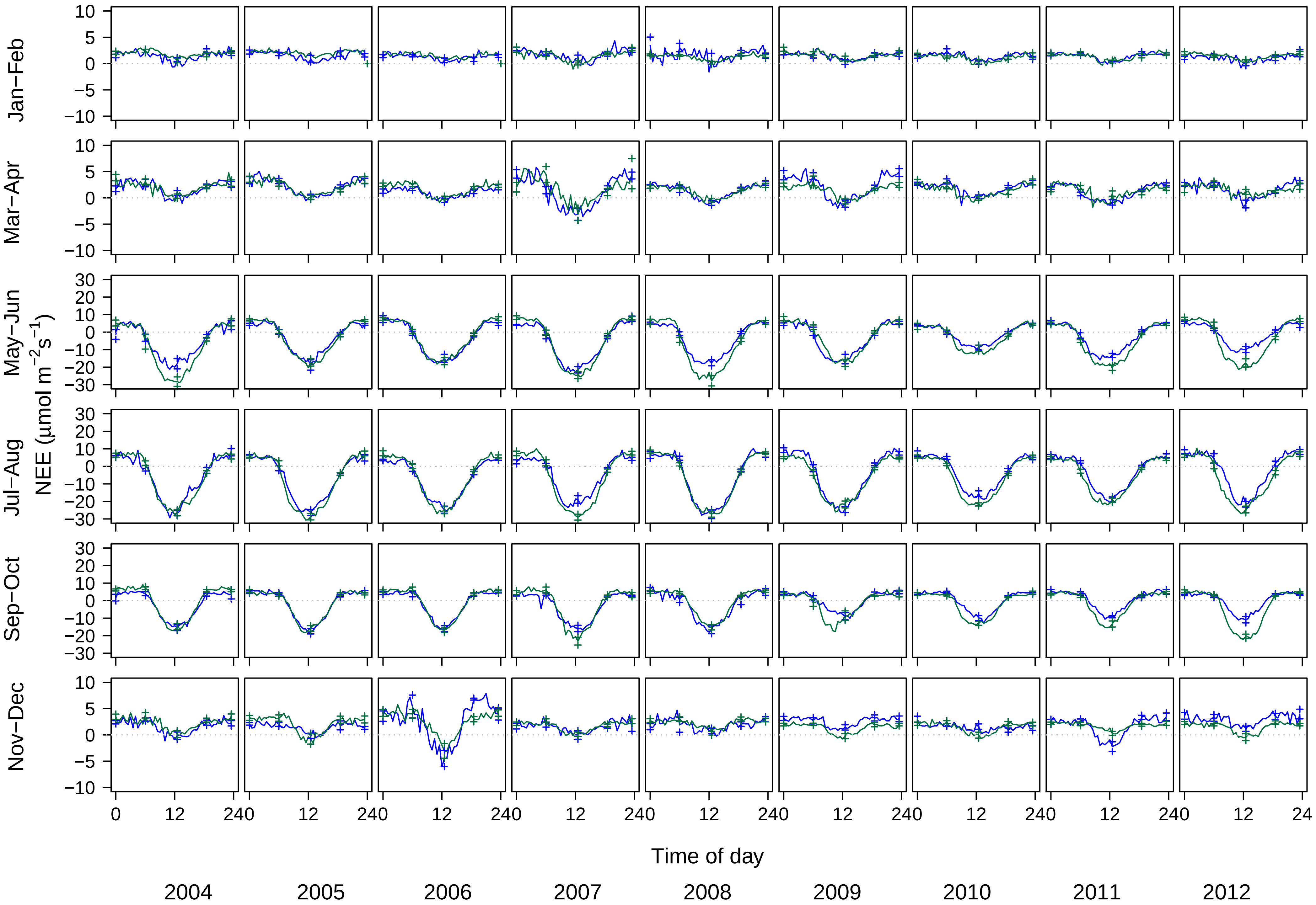

Jan−Feb
Mar−Apr
May−Jun
Jul−Aug
Sep−Oct
Nov−Dec
NEE (μmol m^{-2}s^{-1})
Time of day
2004
2005
2006
2007
2008
2009
2010
2011
2012

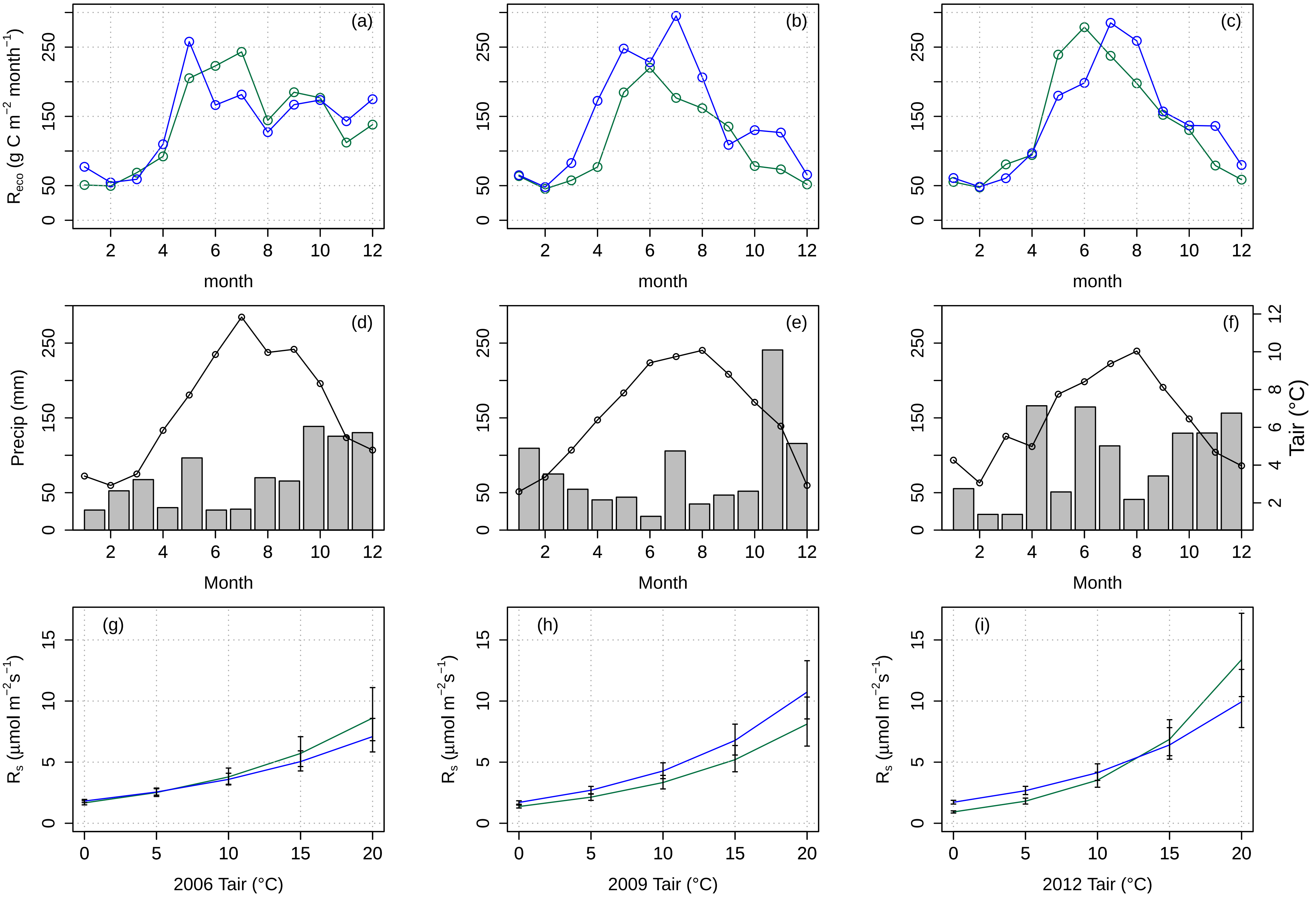

(a)
(b)
(c)
R_{eco} (g C m^{-2} $month^{-1}$)
month
(d)
(e)
(f)
Precip (mm)
Tair (°C)
Month
(g)
(h)
(i)
R_s (µmol $m^{-2}s^{-1}$)
2006 Tair (°C)
2009 Tair (°C)
2012 Tair (°C)

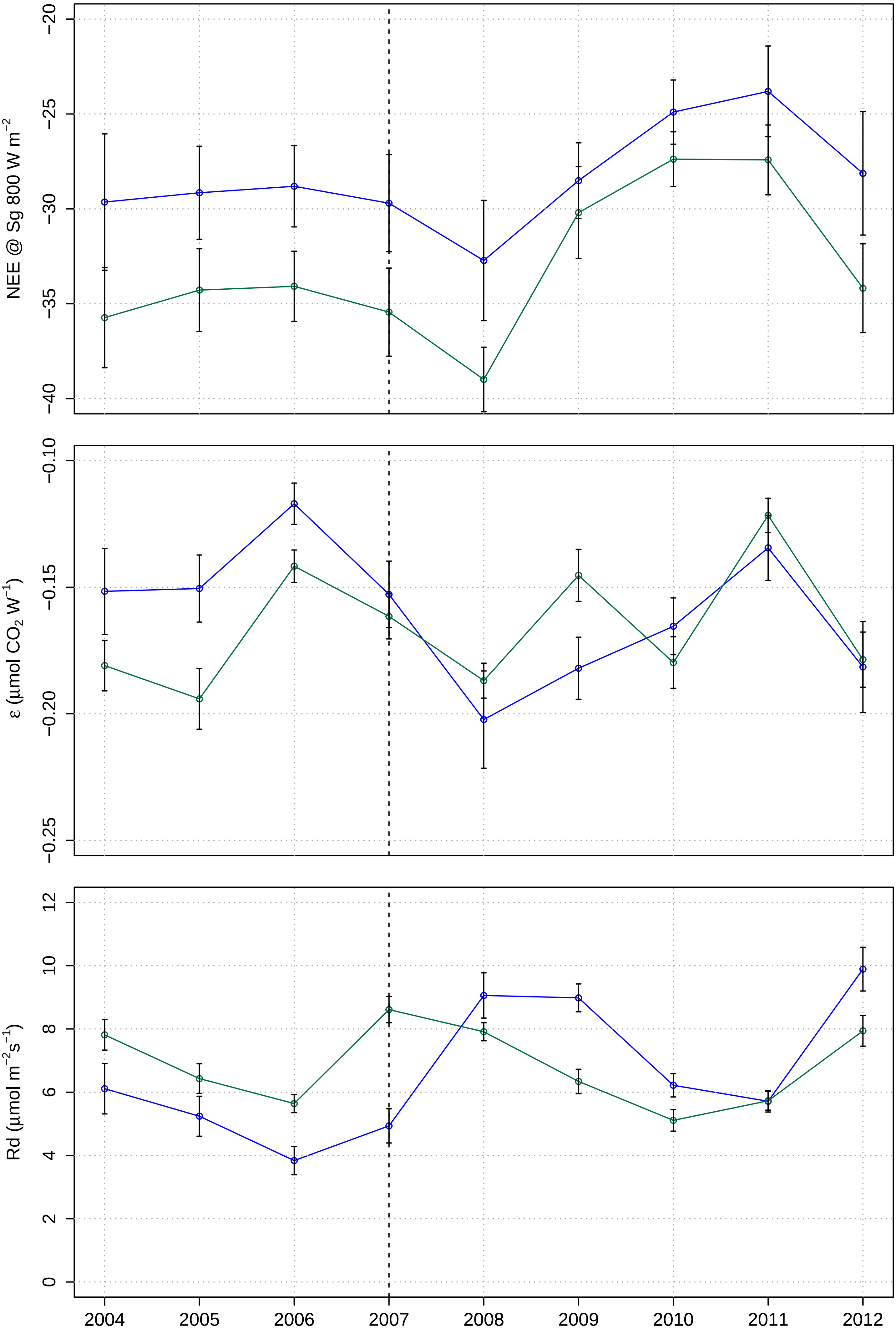

NEE @ Sg 800 W m^{-2}
−20
−25
−30
−35
−40
ε (μmol CO_2 W^{-1})
−0.10
−0.15
−0.20
−0.25
Rd (μmol m^{-2}s^{-1})
12
10
8
6
4
2
0
2004
2005
2006
2007
2008
2009
2010
2011
2012

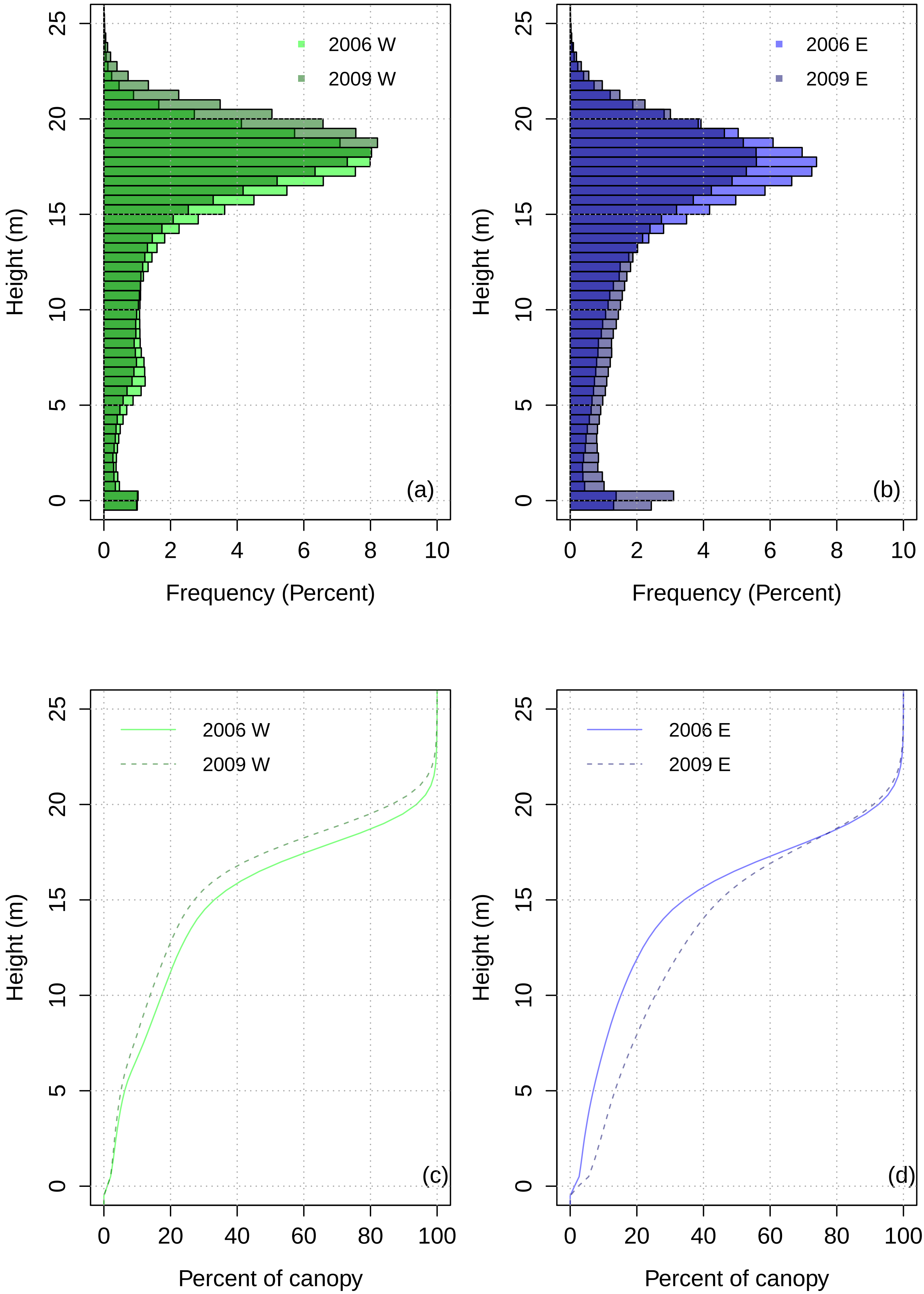
2006 W
2009 W
Height (m)
Frequency (Percent)
(a)
2006 E
2009 E
(b)
Percent of canopy
(c)
(d)